

POINT PROCESS MODELING OF WILDFIRE HAZARD IN LOS ANGELES COUNTY, CALIFORNIA

BY HAIYONG XU AND FREDERIC PAIK SCHOENBERG

University of California, Los Angeles

The Burning Index (BI) produced daily by the United States government's National Fire Danger Rating System is commonly used in forecasting the hazard of wildfire activity in the United States. However, recent evaluations have shown the BI to be less effective at predicting wildfires in Los Angeles County, compared to simple point process models incorporating similar meteorological information. Here, we explore the forecasting power of a suite of more complex point process models that use seasonal wildfire trends, daily and lagged weather variables, and historical spatial burn patterns as covariates, and that interpolate the records from different weather stations. Results are compared with models using only the BI. The performance of each model is compared by Akaike Information Criterion (AIC), as well as by the power in predicting wildfires in the historical data set and residual analysis. We find that multiplicative models that directly use weather variables offer substantial improvement in fit compared to models using only the BI, and, in particular, models where a distinct spatial bandwidth parameter is estimated for each weather station appear to offer substantially improved fit.

1. Introduction. This paper explores the use of space–time point process models for the short-term forecasting of wildfire hazard in Los Angeles County, California. The region is especially well suited to such an analysis, since the Los Angeles County Fire Department and Department of Public Works have collected and compiled detailed records on the locations burned by large wildfires dating back over a century. The landscape in Los Angeles County is uniquely vulnerable to high intensity crown-fires, largely because the predominant local vegetation consists of dense, highly flammable contiguous chaparral shrub [Keeley (2000)]. In addition, the dry summers and early autumns in Los Angeles County are typically followed by high winds

Received April 2009; revised August 2010.

Key words and phrases. Burning index, conditional intensity, point process, residual analysis.

<p>This is an electronic reprint of the original article published by the Institute of Mathematical Statistics in <i>The Annals of Applied Statistics</i>, 2011, Vol. 5, No. 2A, 684–704. This reprint differs from the original in pagination and typographic detail.</p>
--

known locally as Santa Ana winds [Keeley and Fotheringham (2003)]. These offshore winds reach speeds exceeding 100 kph at a relative humidity below 10%, and are annual events lasting several days to several weeks, creating the most severe fire weather in the United States [Schroeder et al. (1964)].

In order to forecast wildfire hazard, the United States National Fire Danger Rating System (NFDRS), created in 1972, produces several daily indices that are designed to aid in planning fire control activities on a fire protection unit [Deeming et al. (1977); Bradshaw et al. (1983); Burgan (1988)]. These include the Occurrence Index, the Burning Index (BI), and the Fire Load Index. These indices are derived from three fire behavior components—a Spread Component, an Energy Release Component, and an Ignition Component, that are in turn computed based on fuel age, environmental parameters (slope, vegetation type, etc.), and meteorological variables such as wind, temperature, and relative humidity. Local wildfire management agencies may combine these components in different ways or calibrate the inherent parameters to adapt the system to the local environment for wildfire hazard assessment.

Fire managers use this information in making decisions about the appropriateness of prescribed burning or alerts for increased preparedness, both in terms of fire suppression staffing and fire prevention activities. Since fire-line intensity is an important factor in predicting fire containment and the likelihood of fire escape, the Burning Index is the rating of most interest to many fire managers [Schoenberg et al. (2010)]. This is especially the case for natural crown-fire ecosystems such as southern California shrublands, where BI is commonly employed to assess fire danger [Mees and Chase (1991)]. Indeed, in Los Angeles County, as well as at least 90% of counties nationwide, the BI is the index primarily used by fire department officials as a measure of overall wildfire hazard, and its use has been justified largely based on its observed empirical correlation with wildfire incidence and burn area in different regions [Haines et al. (1983); Haines, Main and Simard (1986); Mees and Chase (1991); Andrews, Loftsgaarden and Bradshaw (2003)]. However, several recent investigations have shown that the BI is far from an ideal predictor of wildfire incidence in Los Angeles County; Schoenberg et al. (2010) showed that a simple point process model, which used only the same weather variables as those incorporated by the BI, vastly outperformed the BI in terms of predictive efficacy in Los Angeles County, using historical data from 1977–2000. In fact, the simple model in Schoenberg et al. (2010) not only offered improvement in terms of likelihood scores such as the Akaike Information Criterion (AIC), but the study suggested that substantial improvement in short-term forecasting could be achieved by the simple model using the weather variables directly, compared to a point process model that interpolates BI measurements.

Here, we adopt the same basic modeling framework of Schoenberg et al. (2010), but extend the models in two important ways. First, we consider not only daily weather variables but also additional covariates with management relevance, such as historical spatial burn patterns and wind direction, using the directional kernel regression method described in Schoenberg and Xu (2008). Second, unlike the simple models of Mees and Chase (1991) and Schoenberg et al. (2010) that average daily weather variables over weather stations within Los Angeles County, here we explore models that interpolate the records from different weather stations, weighting these data based on their spatial distance from the location where wildfire hazard is to be estimated. Thus, the models considered here should have more direct relevance for forecasting wildfire hazard in precise spatial locations within Los Angeles County, compared to previous work that essentially averaged weather variables and hazard estimates over Los Angeles County as a whole. As with Schoenberg et al. (2010), our results are compared with models using the BI measurements recorded at each of the weather stations, so that the effectiveness of the BI in summarizing the wildfire hazard as a function of the weather variables may be assessed.

While alternative models may be more useful for forecasting long-term wildfire hazard, that is, estimating the number of wildfires occurring within a month, season, or year, the focus here is on forecasting short-term wildfire hazard, that is, the probability of a wildfire occurring within a specific day. To compare the overall performance of the models considered, we employ diagnostics including likelihood-based numerical summaries such as the Akaike Information Criterion (AIC), as well as power diagrams summarizing the predictive efficacy of each model for short-term forecasting. Residual analysis is also used to highlight specific areas and times where the performance of a model is poor and to suggest areas for improvement.

The paper proceeds as follows. Section 2 describes the wildfire and weather data that are used in the analysis. The models used, as well as methods for their estimation, are outlined in Section 3, and methods for goodness-of-fit assessment are discussed in Section 4. Section 5 presents the main results, and a discussion is given in Section 6.

2. Data.

2.1. *Wildfire data.* Los Angeles County is an ideal test site for models for wildfire hazard, with detailed wildfire data having been collected and compiled by various agencies, including the Los Angeles County Fire Department (LACFD) and the Los Angeles County Department of Public Works, the Santa Monica Mountains Recreation Area, and the California Department of Forestry and Fire Protection. Regional records of the occurrence of wildfires date back to 1878, and include information on each fire,

including its origin date, the polygonal outline of the resulting area burned, and the centroidal location of this polygon. LACFD officials have noted that the records prior to 1950 are believed to be complete for fires greater than 0.405 km^2 (100 acres), and data since 1950 are believed to be complete for fires burning greater than 0.0405 km^2 , or 10 acres [Schoenberg et al. (2003)]. As in Schoenberg et al. (2010), our analysis in this paper is focused primarily on models for the occurrences of the 592 wildfires burning at least 0.0405 km^2 recorded between January 1976 and December 2000. The daily burn area is highly right-skewed and closely follows the tapered Pareto distribution [Schoenberg, Peng and Woods (2003)]. For further details, images of the spatial locations of these wildfires, and information about missing data, see Peng, Schoenberg and Woods (2005).

2.2. Meteorological data. Since 1976, daily meteorological observations from the Remote Automatic Weather Stations (RAWS) were archived across the United States. The analysis here is based on sixteen RAWS located within Los Angeles County, California. The RAWS record daily measures of many meteorological variables, including air temperature, relative humidity, precipitation, wind speed, and wind direction [Warren and Vance (1981)]. Summaries of these records are collected daily at 1300 hr and transmitted by satellite to a central archiving station. These daily RAWS data are used as inputs by the NFDRS in order to construct fire behavior components that are in turn combined to construct the BI. It should be noted that data were missing on certain days for several of the 16 RAWS, though the biases resulting from such missing data are likely to be small; see Peng, Schoenberg and Woods (2005) for details.

3. Methodology. We follow previous research including Schoenberg et al. (2010) in modeling the catalog of wildfire centroids in Los Angeles County as a realization of a point process that may depend on daily meteorological variables. We begin with a basic reference model using merely a spatial background rate and seasonal component, and a model using the Burning Index in addition to the spatial and seasonal background rates. We then introduce competing models that use daily meteorological variables recorded at the RAWS, and extend the research of Schoenberg et al. (2010) by including additional covariates, such as wind direction and fuel age. Further, instead of averaging daily weather variables or the Burning Index over all weather stations within Los Angeles County, here we explore methods of obtaining an estimated spatial intensity at any location x on any particular day by interpolating the meteorological variables from different weather stations, weighting each record based on its distance from the location x in question.

3.1. *A review of point process modeling.* A spatial-temporal point process N is mathematically defined as a random measure on a spatial-temporal region S , taking values in the nonnegative integers \mathbb{Z}^+ or infinity [Daley and Vere-Jones (2003)]. In this framework the measure $N(A)$ represents the number of points falling in the subset A of S . Since any analytical spatial-temporal point process is characterized uniquely by its associated conditional rate (or intensity) $\lambda(s)$, assuming it exists, modeling of such point processes is typically performed by specifying a parametric model for this rate. For the case where the spatial region is planar, for any point t in time and location (x, y) in the plane, the conditional rate is defined as a limiting frequency at which events are expected to occur within time range $(t, t + \Delta t)$ and rectangle $(x, x + \Delta x) \times (y, y + \Delta y)$, conditional on the prior history, H_t , of the point process up to time t . For references on space-time point processes and conditional rates, see, for example, Daley and Vere-Jones (1988) or Schoenberg, Brillinger and Guttorp (2002).

Given a parametric function for $\lambda(t, x, y)$, estimates of the parameters θ may be obtained by maximizing the log-likelihood function [see Schoenberg, Brillinger and Guttorp (2002), page 1576, or Daley and Vere-Jones (2003), page 232, equation 7.24]:

$$\begin{aligned} L(\theta) &= \int_{T_0}^{T_1} \int_x \int_y \log[\lambda(t, x, y; \theta)] dN(t, x, y) - \int_{T_0}^{T_1} \int_x \int_y \lambda(t, x, y; \theta) dy dx dt \\ &= \sum_{i=1}^n \log \lambda(t_i, x_i, y_i; \theta) - \int_{T_0}^{T_1} \int_x \int_y \lambda(t, x, y; \theta) dy dx dt. \end{aligned}$$

In the case of a Poisson process, the intuition behind this formula is that $\prod_{i=1}^n \lambda(t_i, x_i, y_i; \theta)$ reflects the likelihood associated with the observed events, and $\exp\{-\int_{T_0}^{T_1} \int_x \int_y \lambda(t, x, y; \theta) dy dx dt\}$ represents the probability of no events in any *other* portions of the spatial-temporal region, the full likelihood is the product of these two terms, and the logarithm of this product yields $L(\theta)$ above. Under rather general conditions, the maximum likelihood estimates (MLEs) are consistent, asymptotically normal, and efficient [Ogata (1978)], and estimates of their variance can be derived from the negative of the diagonal elements of the inverse Hessian of the likelihood function [Ogata (1978), Rathbun and Cressie (1994)]. In most cases, explicit solutions for MLEs are not available and iterative numerical optimization methods are used instead.

3.2. *A simple reference model.* In this analysis we explore several spatial-temporal point process models for predicting wildfire occurrence rates. As an initial baseline model, one may consider an inhomogeneous Poisson process, where the conditional intensity at time t and at location (x, y) depends only

on the season associated with time t , as well as the background rate $m(x, y)$ of wildfires for the location in question. That is, one may consider a baseline model such as

$$(1) \quad \lambda_1(t, x, y) = \gamma m(x, y) + \alpha S(t),$$

where γ and α are parameters to be estimated in modeling fitting.

Parametric or nonparametric methods can be used to estimate the seasonal pattern $S(t)$ and spatial background $m(x, y)$. While nonparametric methods can be especially flexible for estimating complex patterns such as spatial burn averages, a possible drawback to such methods is their potential for overfitting, particularly when the same data are used for fitting and evaluation of the fit of the model. As in Schoenberg et al. (2010), we propose estimating the spatial background $m(x, y)$ for fires between 1976–2000 by kernel smoothing the centroidal locations of wildfires recorded during the previous 25 years, that is, from January 1950 to December 1975. That is,

$$m(x, y) = \frac{1}{n_0 \beta_m} \sum_{j=1}^{n_0} K\left(\frac{\|(x, y) - (x_j, y_j)\|}{\beta_m}\right),$$

where K is a kernel function, β_m is a bandwidth to be estimated in modeling fitting, (x_j, y_j) indicates the spatial coordinates of the j th wildfire between 1950 and 1975, n_0 is the number of observed 1951–1975 wildfire occurrences, and $\|(x, y) - (x_j, y_j)\|$ is the Euclidian distance between (x, y) and (x_j, y_j) . Standard kernel functions can be used, and attention is usually limited to functions that are unimodal, symmetric about zero, and that integrate to 1, such as the Gaussian density of the Epanechnikov kernel [Härdle (1994)]. It is well known that the results are far more sensitive to the choice of bandwidth than the choice of kernel function, and much research has focused on automated methods for choosing bandwidth parameters, including cross-validation, penalty functions, and plug-in methods [Silverman (1986); Härdle (1994)]. Here, since the data (x_j, y_j) used in the estimation of $m(x, y)$ is distinct from that used in the rest of the model fitting and in the evaluation, the problem of overfitting is far less severe, and the bandwidth parameter may simply be fitted by maximum likelihood.

Figure 1 shows an estimate of the spatial background rate $m(x, y)$, with bandwidth estimated by maximum likelihood. One sees the general pattern of fire activity in Los Angeles County during 1951–1975, with most fires occurring in the Angeles National Forest, as well as parts of the Los Padres National Forest and the Santa Monica Mountains, while many other wildfires were located in or near Buckweed, Santa Clarita, and Glendale, California.

Helmers, Magku and Zitikis (2003) propose a kernel-based estimate for the consistent estimation of a seasonal time series. Here, in order to safeguard against overfitting, we propose estimating the seasonal pattern $S(t)$

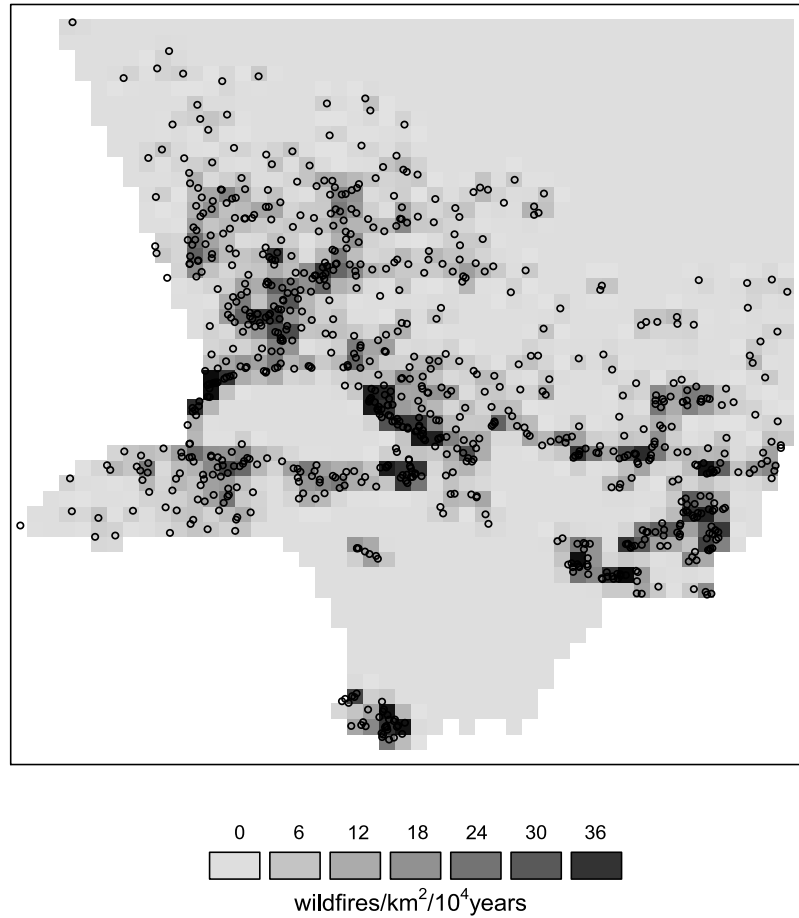


FIG. 1. Spatial background rate $m(x, y)$, with centroid locations of wildfires occurring during 1878–1976. (The spatial bandwidth β_m is 0.6 miles).

describing the overall seasonal variation of wildfire activity in a fashion similar to that used for the spatial background rate, that is, by kernel smoothing the times of wildfires during *previous* years:

$$S(t) = \frac{1}{n_0 \beta_t} \sum_{j=1}^{n_0} K\left(\frac{T^*(t) - T^*(t_j)}{\beta_t}\right).$$

In the above equation, $T^*(t)$ represents the date within the year associated with time t , that is, $T^*(t)$ is the number of days since the beginning of the year for time t , t_j is the time of the j th wildfire occurrence in the data set (1950–1975), and β_t is a bandwidth parameter to be estimated. A wrapped kernel function K should be used so that, for instance, January 1 and December 31 are treated as one day apart. The bandwidth may be

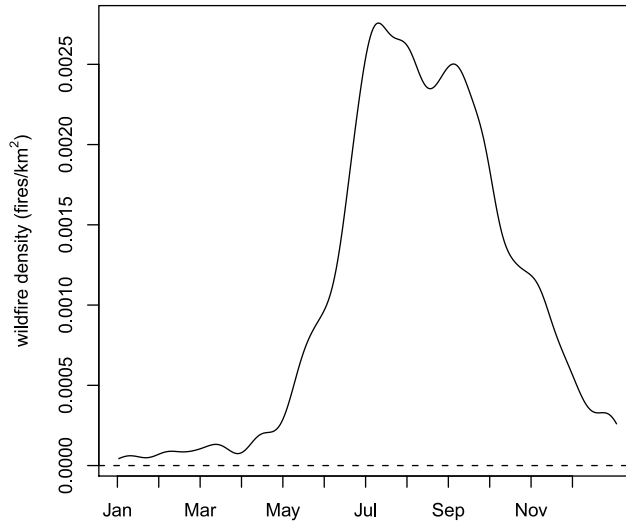


FIG. 2. Estimate of the seasonal pattern $S(t)$ for model (1), using kernel regression with a wrapped Gaussian kernel and bandwidth $\hat{\beta}_t = 9.86$ days, estimated by MLE.

estimated by maximum likelihood, fitting the kernel smoothing of the 1950–1975 data to the 1976–2000 data set. This procedure may be preferable for relatively small data sets such as the one considered here in order to prevent overfitting.

Figure 2 displays the smoothed function $S(t)$ applied to wildfire incidence in Los Angeles County from January 1950 to December 1975, with bandwidth estimated by MLE by fitting the resulting function to wildfire data from 1976–2000. It is evident that the mean number of wildfires is highest between July and October and rapidly decreases during November and December, reaching its minimum in January and February. Schoenberg et al. (2010) pointed out that the Burning Index typically assumes moderate values in December, January, and February, though few wildfires occur during these months.

3.3. *A point process model using Burning Index.* To evaluate the potential of the Burning Index (BI) in predicting wildfire incidence, one may consider a model such as

$$(2) \quad \lambda_2(t, x, y) = \gamma m(x, y) + \alpha S(t) + \mu_{\text{BI}} B(t, x, y)$$

for some function $B(t, x, y)$ which interpolates the BI records at time t and location (x, y) , since BI records are only available at fixed RAWS sites. Different methods of interpolation are possible. One possibility is to average the BI records on day t , weighing each by the distance between the RAWS

and the location (x, y) in question. That is,

$$B(t, x, y) = \frac{1}{C_{\text{BI}}} \sum_{s \in S_t} \left\{ K \left(\frac{\|(x, y) - (x_s, y_s)\|}{\beta_{\text{BI}}} \right) \text{BI}(t, s) \right\},$$

where $\text{BI}(t, s)$ is the BI value recorded at time t from the s th station, (x_s, y_s) are the coordinates of the s th station, S_t represents the collection of stations for which BI records are available on day t , and C_{BI} is a normalizing constant given by

$$C_{\text{BI}} = \sum_{s \in S_t} \left\{ K \left(\frac{\|(x, y) - (x_s, y_s)\|}{\beta_{\text{BI}}} \right) \right\}.$$

3.4. *Models using spatial interpolation of meteorological variables, including wind speed and wind direction.* As an alternative to the model (2) incorporating BI measurements, one may instead consider examining the direct impact on wildfire hazard estimates of meteorological variables used in the computation of the BI, by replacing the function $B(t, x, y)$ in (2) by functions of the meteorological variables themselves. That is, one may consider models such as

$$(3) \quad \lambda_3(t, x, y) = \gamma m(x, y) + \alpha S(t) + F_1(t, x, y),$$

where $F_1(t, x, y)$ takes into account the contribution of temperature (T), relative humidity (H), wind speed (W), and precipitation (P) at time t from each RAWS where the data are available.

Since nonlinearities have been detected in the dependence of burn area on climatic variables [Schoenberg et al. (2003)], one may wish to avoid simple averaging of the meteorological variables in estimating wildfire hazard. Instead, one option is to describe the association between each climatic variable and wildfire burn area by an explicit function g and weight the information from each RAWS by the distance to the point (x, y) to be estimated using kernel smoothing. This suggests a model such as

$$\begin{aligned} F_1(t, x, y) &= \frac{\mu_T}{C_T} \sum_{s \in S_t} \left\{ K \left(\frac{\|(x, y) - (x_s, y_s)\|}{\beta_T} \right) g_T(T(t, s)) \right\} \\ &+ \frac{\mu_H}{C_H} \sum_{s \in S_t} \left\{ K \left(\frac{\|(x, y) - (x_s, y_s)\|}{\beta_H} \right) g_H(H(t, s)) \right\} \\ &+ \frac{\mu_W}{C_W} \sum_{s \in S_t} \left\{ K \left(\frac{\|(x, y) - (x_s, y_s)\|}{\beta_W} \right) g_W(W(t, s)) \right\} \\ &+ \frac{\mu_P}{C_P} \sum_{s \in S_t} \left\{ K \left(\frac{\|(x, y) - (x_s, y_s)\|}{\beta_P} \right) g_P(P(t, s)) \right\}, \end{aligned}$$

where $T(t, s)$, $H(t, s)$, $W(t, s)$, and $P(t, s)$ are records of temperature, relative humidity, directed wind speed, and precipitation, respectively, on day t at the s th RAWS, the parameters μ_T, μ_R, μ_W , and μ_P represent weights associated with these meteorological variables, $\beta_T, \beta_H, \beta_W$, and β_P are bandwidths to be estimated, and C_T, C_H, C_W , and C_P are normalizing constants.

Note that the bandwidth parameters are somewhat different here than in ordinary kernel regression models. While ordinarily in kernel regression or kernel density estimation bandwidth parameters may not typically be estimated by maximum likelihood because the likelihood would tend to increase as the bandwidth shrinks to 0 [Silverman (1986)], here this is not the case. Instead, the bandwidth parameters $\beta_T, \beta_H, \beta_W$, and β_P in model (3) merely control the spheres of influence of the relative weather stations in terms of the impact of each on wildfire hazard. That is, if β_T is small, for instance, then each RAWS station's recorded temperature will affect the wildfire incidence more locally, whereas if β_T is very large, then the wildfire hazard at any particular location will depend more closely on the average temperature throughout Los Angeles County.

Functional forms can be suggested for g_T, g_H, g_W , and g_P , by individually examining the empirical relationship between daily area burned and each of these variables. In order to smooth these relationships, one possibility would be to use local linear regression or segmented regression, since the relationships between wildfire burn area and temperature, precipitation, and other weather variables appear to have thresholds [Schoenberg et al. (2003)]. Another possibility is to use kernel regression of daily area burned on the average temperature, relative humidity, and precipitation over all RAWS, respectively. For instance, the impact of temperature may be estimated via

$$g_T(T) = \frac{\sum_{j=1}^{n_1} \{K(|T - T_j|/h_T) A_j\}}{\sum_j \{K(|T - T_j|/h_T)\}},$$

where A_j is the area burned on the j th day during 1976–2000, T_j is the average temperature readings over all RAWS on that day, h_T is the bandwidth of the kernel regression which can be selected by methods such as cross-validation or the plug-in method [Silverman (1986)], and n_1 is the number of days with records during this period. Figure 3 displays such kernel regression estimates of g_T, g_H , and g_P . Not surprisingly, one sees that daily area burned generally increases as temperature increases, and decreases as relative humidity and precipitation increase, though some local fluctuations are seen in the kernel regressions on temperature and relative humidity. These fluctuations are likely attributable to the high variability of the estimates due to the relatively small sample of large fires contained in the catalog.

Special care should be taken in estimating g_W , since wind is directional, and this direction may provide important information related to wildfire

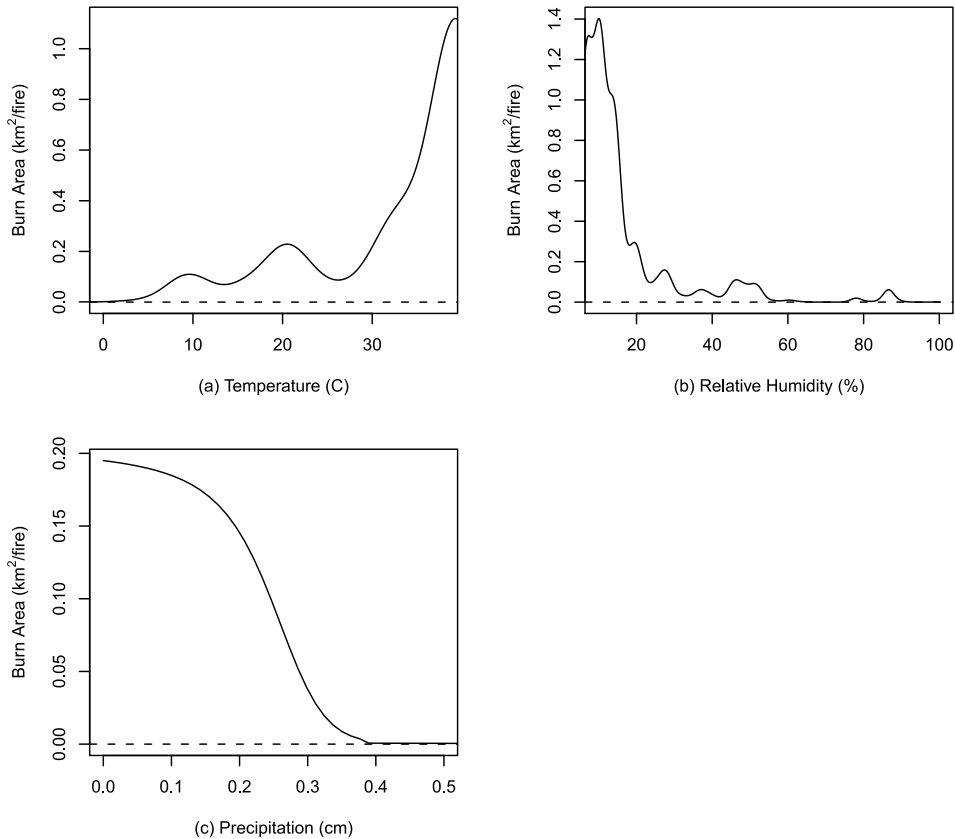


FIG. 3. Kernel regression estimates of the relationship between daily burn area and (a) temperature, (b) relative humidity, and (c) precipitation. Gaussian kernels are used, bandwidths are estimated by cross-validation, and edge correction is performed via reflection [Silverman (1986)].

incidence. One possible way to estimate the relationship between daily area burned and directional wind speed is via directional kernel regression, as outlined in Schoenberg and Xu (2008). An example of a two-dimensional directional kernel is the von Mises distribution suggested by Mardia and Jupp (2000):

$$vM(\theta; \mu, \kappa) = \frac{1}{2\pi I_0(\kappa)} e^{\kappa \cos(\theta - \mu)},$$

where I_0 denotes the modified Bessel function of the first kind and order 0, μ is the directional center, and κ is known as the concentration parameter. Following Schoenberg and Xu (2008), the corresponding two-dimensional

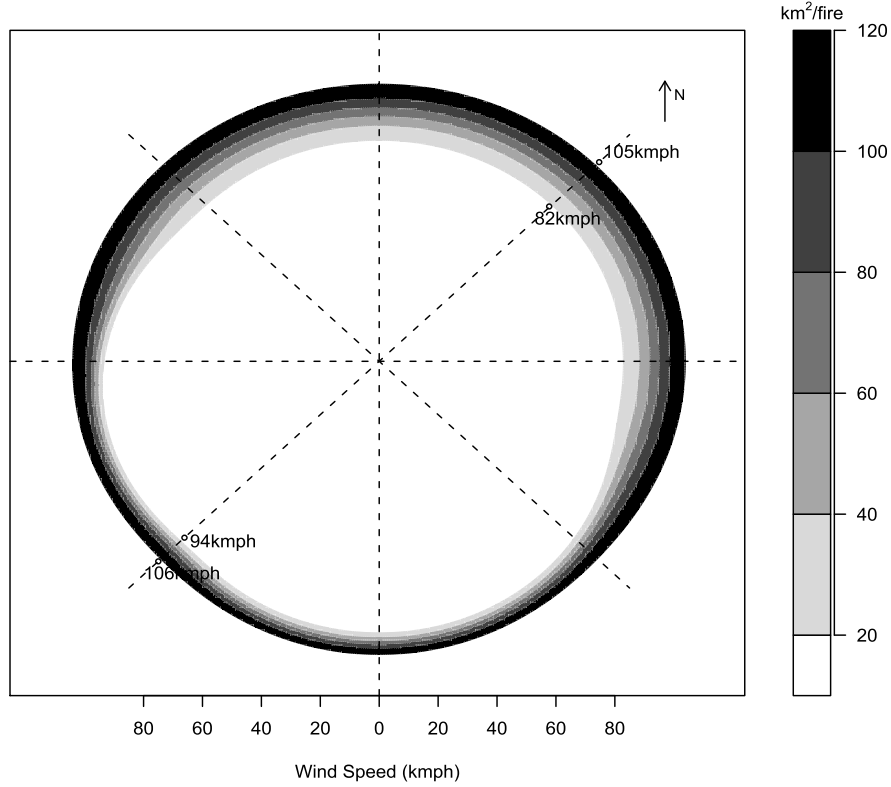


FIG. 4. Two-dimensional kernel regression of burn area versus wind speed and wind direction. Wind speed and wind direction are represented in a polar system: wind speed is represented by the distance to the center and wind direction is represented by the angle. The grey scale represents the smoothed average wildfire burn area during 1976–2000.

kernel regression function g_W would then be estimated via

$$g_W(W, \theta) = \frac{\sum_{j=1}^{n_1} \{K(|W - W_j|/h_W) v M(\theta - \theta_j; \mu_0, \kappa_0) A_j\}}{\sum_{j=1}^{n_1} \{K(|W - W_j|/h_W) v M(\theta - \theta_j; \mu_0, \kappa_0)\}},$$

where W_j and θ_j represent the mean wind speed and wind direction, respectively, on day j . Cross-validation can be used to optimize the estimates of h_{sp} , μ_0 , and κ_0 .

Figure 4 displays a kernel regression estimate of the relationship between daily burning area and daily mean wind direction, weighted by wind speed, averaged over all 16 RAWS stations. The sharp increase in mean wildfire burn area, indicated by darker shading in Figure 4, is very strongly associated with higher wind speeds. In addition, one sees from Figure 4 the extent to which winds from the northeast, which are often warm, dry Santa Ana winds, are associated with higher burn areas. Since the impact on av-

erage wildfire burn area of wind direction might be different at distinct weather stations, one might wish to estimate 16 distinct kernel regression functions $g_W^{(s)}$, one for each RAWS station s .

The model (3) described above is additive in each of the weather variables, implying that an extreme value in only one weather variable may lead to a high estimate of wildfire hazard on the corresponding day, which might be questionable. For instance, one would expect few large wildfires occur on days when temperatures are extremely high yet there is some moderate amount of precipitation and relative humidity. An alternative approach is to use a multiplicative component instead, where once again

$$(4) \quad \lambda_4(t, x, y) = \gamma m(x, y) + \alpha S(t) + \mu F_2(t, x, y),$$

where now the fire weather (F) term has the multiplicative form

$$F_2(t, x, y) = \frac{1}{C_2} \sum_{s \in S_t} \left\{ K \left(\frac{\|(x, y) - (x_s, y_s)\|}{\beta_2} \right) g_T(t, s) g_H(t, s) g_W(t, s) g_P(t, s) \right\}.$$

3.5. *Models allowing records at different RAWS to have different relationships with wildfire hazard.* In both model (3) and model (4), g_T, g_H , and g_P may be estimated using kernel regression of burn area on average temperature, relative humidity, and precipitation over all weather stations, where each station has the same regression function. However, because of differences in the locations of the weather stations, including differing altitudes of these stations, some stations may have lower average temperatures or higher relative humidities than others throughout the year. Hence, a particular temperature and relative humidity at one station might indicate a very different wildfire hazard than the same values observed at a different RAWS station. In order to deal with this, one may estimate distinct kernel regression curves for each RAWS in model (3) and model (4). That is, one might consider

$$(5) \quad \lambda_5(t, x, y) = \gamma m(x, y) + \alpha S(t) + F_3(t, x, y),$$

where

$$\begin{aligned} F_3(t, x, y) &= \frac{\mu_T}{C_T} \sum_{s \in S_t} \left\{ K \left(\frac{\|(x, y) - (x_s, y_s)\|}{\beta_T} \right) g_T^{(s)}(t, s) \right\} \\ &\quad + \frac{\mu_H}{C_H} \sum_{s \in S_t} \left\{ K \left(\frac{\|(x, y) - (x_s, y_s)\|}{\beta_H} \right) g_H^{(s)}(t, s) \right\} \\ &\quad + \frac{\mu_W}{C_W} \sum_{s \in S_t} \left\{ K \left(\frac{\|(x, y) - (x_s, y_s)\|}{\beta_W} \right) g_W^{(s)}(t, s) \right\} \\ &\quad + \frac{\mu_P}{C_P} \sum_{s \in S_t} \left\{ K \left(\frac{\|(x, y) - (x_s, y_s)\|}{\beta_P} \right) g_P^{(s)}(t, s) \right\} \end{aligned}$$

or

$$(6) \quad \lambda_6(t, x, y) = \gamma m(x, y) + \alpha s(t) + \mu F_4(t, x, y),$$

where

$$F_4(t, x, y) = \frac{1}{C} \sum_{s \in S_t} \left\{ K \left(\frac{\|(x, y) - (x_s, y_s)\|}{\beta} \right) g_T^{(s)}(t, s) g_H^{(s)}(t, s) g_W^{(s)}(t, s) g_P^{(s)}(t, s) \right\}.$$

The kernel regression functions such as $g_T^{(s)}(t, s)$ for each station s may be estimated as in models (3) and (4), that is, by kernel regression of the total daily burn area in Los Angeles County against the temperature at station s .

3.6. Incorporating fuel age. One may further improve the models by adding fuel age as a covariate. Fuel age, or its proxy, the time since the location's last recorded burn, appears to have a nonlinear, threshold-type relationship with burn area [Peng and Schoenberg (2008)]. Indeed, burn area appears to increase steadily with fuel age up to ages of approximately 20–30 years [Peng and Schoenberg (2008)]. This suggests incorporating the contribution of fuel age into model (5) by a truncated linear function, that is,

$$(7) \quad \lambda_7(t, x, y) = \gamma m(x, y) + \alpha s(t) + F_3(t, x, y) + \mu_D \min\{D(t, x, y), \psi\},$$

where $D(t, x, y)$ is the fuel age at the space–time pixel (t, x, y) , and where ψ is an upper truncation time. Fuel age may be incorporated similarly into model (6) as well:

$$(8) \quad \lambda_8(t, x, y) = \gamma m(x, y) + \alpha S(t) + \mu F_4(t, x, y) + \mu_D \min\{D(t, x, y), \psi\}.$$

4. Model assessment. Equations (1)–(8) describe eight point process models that may be used to predict wildfire hazard at any time and location within Los Angeles County. In order to compare the performance of these models, one commonly used method is the Akaike Information Criterion (AIC), which is defined as $-2L(\beta) + 2p$, where $L(\beta)$ is the log-likelihood and p is the number of fitted parameters in the model. Smaller values of AIC indicate better fit. The AIC makes a good trade-off between model complexity and overfitting by rewarding a higher likelihood while penalizing the addition of more parameters [Akaike (1977)].

The predictive capacity of competing point process models may also be compared by examining the models' performance on the 1976–2000 wildfire data, as suggested in Schoenberg et al. (2010). Consider a grid of space–time cells, with each cell's center separated by some distance Δd in space and a temporal distance Δt , and let these cells represent locations and times where alarms may potentially be issued. For any such space–time point

(t, x, y) , one may compute the estimated conditional intensity $\hat{\lambda}(t, x, y)$ for a particular model. Consider issuing an alarm if the value of $\hat{\lambda}(t, x, y)$ is above some certain threshold. We say the alarm is successful if a wildfire occurs within the cell; otherwise, it is a false alarm. The false positive rate of the alarms, defined as the proportion of cells without wildfires where $\hat{\lambda}$ exceeded the alarm threshold, can be compared to the true positive rate, that is, the proportion of wildfires occurring in cells where $\hat{\lambda}$ exceeded the alarm threshold, using traditional Receiver Operating Characteristic (ROC) curves. Each possible alarm threshold represents a single point on the ROC curve, and the resulting curve summarizes the potential efficacy of a model in forecasting wildfires.

While numerical likelihood scores such as AIC and ROC curves can be useful in evaluating the overall performance of a point process model, neither method is useful at identifying particular times and locations where a model fits poorly or suggesting ways in which a model might be improved. For these purposes, it is useful to inspect plots of residuals, which may be defined as the difference between the number of events occurring in a certain space–time interval and the integral of the estimated conditional intensity over the same interval [Baddeley et al. (2005)]. Negative residuals indicate overestimates of wildfire hazard, and very large residuals indicate places and times where the model underestimated wildfire hazard.

5. Results. The maximum likelihood estimates of the parameters for the models (1)–(8) are listed in Tables 1 and 2. In Tables 1 and 2, the parameter ψ was fixed at 22 years for models 7 and 8, based on Peng and Schoenberg (2008); this parameter was also fit by maximum likelihood, yielding very similar results, so, for simplicity, here we report the fit of the model with ψ fixed at 22 years. The bandwidths in spatial background β_m range from 0.25 km to 1.20 km and the bandwidth in the seasonal component fall within 8.6 to 34.1 days. The bandwidths related to spatially kernel smoothing the weather variables range from 0.024 km to 0.40 km in models (3), (5), and (7), with the smallest value for wind speed in model (7) and the largest value corresponding to relative humidity in model (3). As mentioned in Section 3, these bandwidths can perhaps be interpreted as reflecting the scales of influence of the weather variables in terms of their effect on wildfire incidence.

Table 3 presents the relative AIC values for models (1)–(8). For simplicity and ease of presentation, the AIC for the best fitting model (8) has been subtracted from the AIC of each model. It is evident that the BI model (2) offers very substantial improvement over the baseline model (1). However, all the other models that use weather information directly have much better fits than the BI model (2). The multiplicative model (8) with fuel age appears to offer by far the best fit among these models, without using the BI directly, and only involves one more fitted parameter than the BI model.

TABLE 1
Maximum likelihood estimates of scaling parameters

Model	γ	α	μ_B	μ_T	μ_H	μ_W	μ_P	μ	μ_D
(1)	24 (1.3)	2.0 (0.20)							
(2)	4.9 (0.26)	0.65 (0.039)	8.6×10^{-4} (2.0×10^{-5})						
(3)	6.4 (0.64)	0.66 (0.043)		0.18 (0.017)	0.21 (0.012)	1.0 (0.071)	0.15 (0.010)		
(4)	6.4 (0.31)	2.7 (0.24)						2.1×10^3 (130)	
(5)	13 (0.84)		0.60 (0.051)	0.58 (0.054)	0.19 (0.011)	17 (0.85)	2.1 (0.14)		
(6)	12 (0.15)	1.0 (0.057)						5.1×10^3 (260)	
(7)	6.9 (0.44)	0.60 (0.054)		0.19 (0.018)	0.21 (0.020)	52 (2.4)	0.71 (0.068)		1.0 (0.066)
(8)	4.8 (0.37)	0.54 (0.049)						1980×10^3 (85×10^3)	0.10 (0.0094)

All entries have been multiplied by 10^3 for brevity.

Figure 5 shows a comparison of the predictive efficacy of models described in Section 3. Models (6) and (8) vastly outperform the other models. The performance was evaluated using a regular space–time grid, so that each alarm’s success or failure was evaluated over a space–time window with $\Delta d = 4.0$ km and $\Delta t = 1.0$ day.

TABLE 2
Maximum likelihood estimates of bandwidth parameters

Model	β_m (km)	β_t (day)	β_B (km)	β_T (km)	β_H (km)	β_W (km)	β_P (km)	β (km)
(1)	1.20 (0.004)	9.86 (2.8)						
(2)	0.92 (0.00077)	8.64 (3.30)	0.40 (0.0055)					
(3)	0.36 (0.002)	29.6 (5.6)		0.37 (0.002)	0.40 (0.001)	0.30 (0.004)	0.24 (0.001)	
(4)	0.92 (0.1)	8.6 (2.3)						0.03 (0.003)
(5)	0.34 (0.002)	34 (8.3)		0.31 (0.001)	0.20 (0.001)	0.04 (0.002)	0.28 (0.0005)	
(6)	0.25 (0.025)	20 (9.7)						0.19 (0.003)
(7)	0.46 (0.00069)	19 (5.2)		0.36 (0.00071)	0.39 (0.0011)	0.024 ($3.2e-8$)	0.20 (0.00025)	
(8)	0.99 (0.17)	13 (2.6)						0.037 (0.00064)

TABLE 3
Relative AIC values

Model	(1)	(2)	(3)	(4)	(5)	(6)	(7)	(8)
Relative AIC	3783	2859	2509	2631	2223	2209	1308	0
p	4	6	12	6	12	6	13	7

For any given success rate, the models that directly use the meteorological data offer substantially fewer false alarms than the model (2) that uses the BI. For instance, for a false positive rate fixed at 0.08, model (8) correctly signals approximately 29% of the wildfires in the data set, compared to 18% for model (2). Model (6), which uses only temperature, relative humidity, wind speed, wind direction, and precipitation, but does not use fuel age, signals nearly 25% of the wildfires correctly with a false positive rate of 0.08. Note that this method of evaluating predictive efficacy over a fine grid of spatial-temporal locations is rather cumbersome for models (7)–(8), due to the need to individually estimate the fuel age associated with each wildfire, with respect to each spatial-temporal grid location and time, and each such evaluation requires a rather burdensome computation described in Peng and Schoenberg (2008).

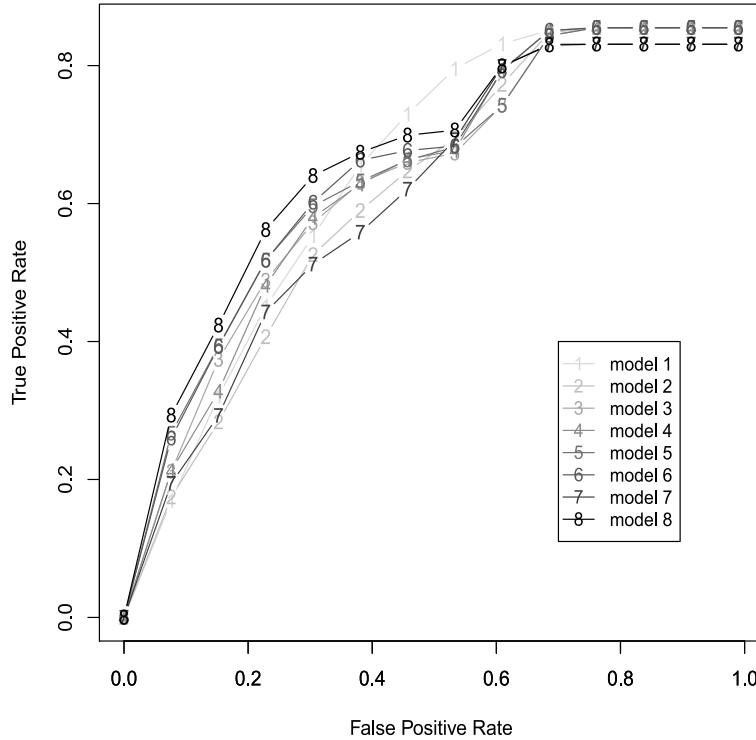


FIG. 5. ROC curves for models (1)–(8), with $\Delta_t = 1.0$ day and $\Delta d = 4.0$ km.

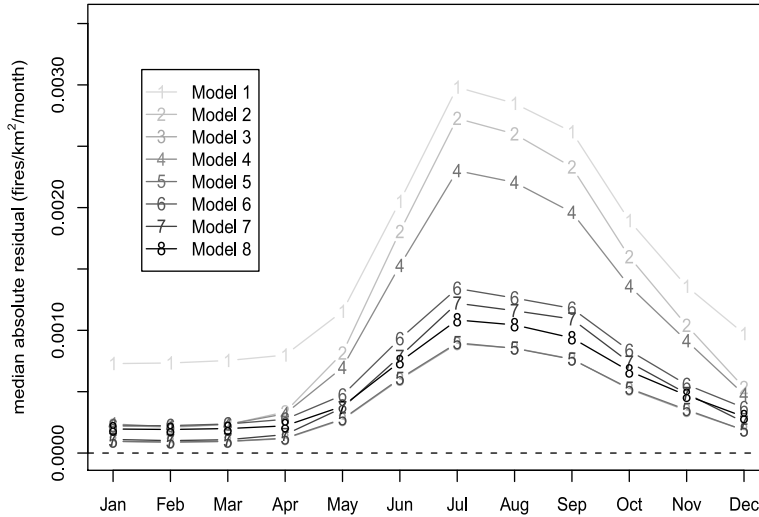


FIG. 6. Median absolute value of residuals, by month, using a space-time grid of $25.6 \text{ sqkm} \times 30.0 \text{ days}$.

The fit of the models can be evaluated by examining their spatial-temporal residuals over a relatively coarse grid. For instance, Figure 6 shows the medians of the absolute values of the residuals in each month, for models (1)–(8), where each residual is computed over a space-time grid of $25.6 \text{ sqkm} \times 30.0 \text{ days}$. It is evident that models (3), (5), (6), (7), and (8) outperform the other three models, especially in the late Summer and Fall months when most wildfires in Los Angeles County occur. The months of October and November are especially critical, since Santa Ana winds prevail and can cause catastrophic wildfires. Figure 7 shows a spatial plot of the medians of the absolute values of the residuals, over all months. From Figure 7 one sees that the eight models perform surprisingly comparably in terms of the median absolute residual, though models (3)–(8), which use meteorological data directly, have better performance than model (2) in the sense that the corresponding residuals are generally closer to zero in most areas. These residual plots also indicate that several of the models may require improvement in the Northwest portion of the Angeles National Forest, as well as near the border with San Bernardino County on the Eastern side of Los Angeles County. From the residuals in Figure 7, one can observe that the residuals for models (5), (7), and (8) are highly concentrated around zero except a few large values that occur in the Northwest part and east part of Los Angeles County.

6. Discussion. The models explored here use the identical information recorded at the RAWS stations and used as inputs into the computation of the BI. Hence, it seems relevant to compare the fit of such models with



FIG. 7. Median absolute value of residuals, by location, using a space-time grid of $25.6 \text{ sqkm} \times 30.0 \text{ days}$.

comparable spatial interpolations of BI measurements, and the fact that the models using the weather variables directly appear to offer superior fit suggests that the BI may not be effective as a short-term forecasting measure of wildfire hazard in Los Angeles County.

It should be noted that the empirical relationship between a fire danger rating index such as the BI and wildfire incidence is only one way to evaluate the effectiveness of such an index; alternatives may include assessing the cost-effectiveness of staffing or other decisions made based on the index. Furthermore, the use of fire danger ratings by fire department officials for

wildfire suppression and prevention activities may confound the empirical relationship between fire danger ratings and observed wildfire activity. Nevertheless, most evaluation studies of fire danger rating systems relate such indices to ultimate fire responses, including fire incidence and fire size. Indeed, Andrews and Bradshaw (1997), whose work was instrumental in the current implementation of the BI, suggested that the value of a fire danger index be evaluated according to its relationship with fire activity, which may be defined as the incidence of large wildfires. Such empirical relationships have been used as support for the use of such rating systems for predictive purposes [Haines et al. (1983); Haines, Main and Simard (1986); Mees and Chase (1991); Mandallaz and Ye (1997a, 1997b); Viegas et al. (1999); Andrews, Loftsgaarden and Bradshaw (2003)]. The results here suggest that, for the purpose of forecasting wildfire hazard, point process models using RAWs records and previous wildfire activity as covariates may represent a promising alternative to existing indices that use essentially the same information.

However, we must emphasize that the point process models proposed here remain rather simplistic and could potentially be improved by incorporating a host of other important variables, such as detailed vegetation type, vegetation cover, soil characteristics, other weather variables such as cloud cover and lightning, as well as human factors such as land use and public policy. The exclusion of such variables from this analysis is solely motivated by our aim to optimize forecasts given the same remote, automatically-recorded information used in the computation of the BI. The models considered here could also perhaps be improved in various ways. For instance, one might allow long-term temporal trends and/or allow the seasonal component to vary from year to year. In addition, one may consider estimating the kernel function in models (5) and (6) for each station using only local wildfires close to the corresponding station, or perhaps by some more sophisticated weighting scheme where nearby fires are given higher weight in the estimation of this function. Because daily burn areas are right-skewed [Schoenberg, Peng and Woods (2003)], perhaps kernel regressions where the response variable is some transformation of the daily burn area might yield superior results. An additional important direction for future work is the exploration of similar point process models for wildfire occurrences in other locations and for other vegetation types or alternative wildfire regimes, as well as the use of such models for actual *prospective* predictions of wildfire activity, rather than merely the empirical assessment of goodness of fit to historical data.

Acknowledgments. Thanks to Larry Bradshaw at the USDA Forest Service for generously providing us with RAWs data and helping us to process it. Thanks also to James Woods, Roger Peng, and members of the LACFD and LADPW (especially Mike Takeshita, Frank Vidales, and Herb Spitzer) for sharing their data and expertise.

REFERENCES

- AKAIKE, H. (1977). On entropy maximization principle. In *Applications of Statistics* (P. R. Krishnaiah, ed.) 27–41. North-Holland, Amsterdam. [MR0501456](#)
- ANDREWS, P. L. and BRADSHAW, L. S. (1997). FIRES: Fire Information Retrieval and Evaluation System—a program for fire danger rating analysis. Gen. Technical Report INT-GTR-367. Ogden, UT; U.S. Dept. Agriculture, Forest Service, Intermountain Research Station. 64 p.
- ANDREWS, P. L., LOFTSGAARDEN, D. O. and BRADSHAW, L. S. (2003). Evaluation of fire danger rating indexes using logistic regression and percentile analysis. *Int. J. Wildland Fire* **12** 213–226.
- BADDELEY, A., TURNER, R., MØLLER, J. and HAZELTON, M. (2005). Residual analysis for spatial point processes (with discussion). *J. Roy. Statist. Soc. Ser. B* **67** 617–666. [MR2210685](#)
- BRADSHAW, L. S., DEEMING, J. E., BURGAN, R. E. and COHEN, J. D. (1983). *The 1978 National Fire-Danger Rating System: Technical Documentation*. United States Dept. Agriculture Forest Service General Technical Report INT-169. Intermountain Forest and Range Experiment Station, Ogden, Utah. 46 p.
- BURGAN, R. E. (1988). 1988 revisions to the 1978 National Fire-Danger Rating System. USDA Forest Service, Southeastern Forest Experiment Station, Research Paper SE-273.
- DALEY, D. and VERE-JONES, D. (1988). *An Introduction to the Theory of Point Processes*. Springer, New York. [MR0950166](#)
- DALEY, D. and VERE-JONES, D. (2003). *An Introduction to the Theory of Point Processes. Vol. 1: Elementary Theory and Methods*. Springer, New York. [MR1950431](#)
- DEEMING, J. E., BURGAN, R. E. and COHEN, J. D. (1977). *The National Fire-Danger Rating System — 1978*. Technical Report INT-39, USDA Forest Service, Intermountain Forest and Range Experiment Station.
- HAINES, D. A., MAIN, W. A., FROST, J. S. and SIMARD, A. J. (1983). Fire-danger rating and wildfire occurrence in the Northeastern United States. *Forest Science* **29** 679–696.
- HAINES, D. A., MAIN, W. A. and SIMARD, A. J. (1986). Fire-danger rating observed wildfire behavior in the Northeastern United States. Res. Pap. NC-274. St. Paul, MN: U.S. Dept. Agriculture, Forest Service, 23 p.
- HÄRDLE, W. (1994). *Applied Nonparametric Regression*. Cambridge, Cambridge University Press.
- HELMERS, R., MAGKU, I. W. and ZITIKIS, R. (2003). Consistent estimation of the intensity function of a cyclic Poisson process. *J. Multivariate Anal.* **84** 19–39. [MR1965821](#)
- KEELEY, J. E. (2000). *Chaparral. P. 203–253 in North American Terrestrial Vegetation*, 2nd ed. (M. G. Barbour and W. D. Billings, eds.). Cambridge University Press, Cambridge.
- KEELEY, J. E. and FOTHERINGHAM, C. J. (2003). Impact of past, present, and future fire regimes on North American Mediterranean shrublands. In: *Fire and Climatic Change in Temperate Ecosystems of the Western Americas* (T. T. Veblen, W. L. Baker, G. Montenegro and T. W. Swetnam, eds.) 218–262. Springer, New York.
- MANDALLAZ, D. and YE, R. (1997a). A new dryness index and the non-parametric estimate of forest fire probabilities. *Schweiz. Z. Forstwes.* **148** 809–822.
- MANDALLAZ, D. and YE, R. (1997b). Prediction of forest fires with Poisson models. *Can. J. For. Res.* **27** 1685–1694.
- MARDIA, K. V. and JUPP, P. E. (2000). *Directional Statistics*. Wiley, New York. [MR1828667](#)
- MEES, R. and CHASE, R. (1991). Relating burning index to wildfire workload over broad geographic areas. *Int. J. Wildland Fire* **1** 235–238.

- OGATA, Y. (1978). The asymptotic behaviour of maximum likelihood estimators for stationary point processes. *Ann. Inst. Statist. Math.* **30** 243–261. [MR0514494](#)
- PENG, R. and SCHOENBERG, F. P. (2008). Estimating fire interval distributions using coverage process data. *Environmetrics*. Unpublished manuscript.
- PENG, R. D., SCHOENBERG, F. P. and WOODS, J. (2005). A space–time conditional intensity model for evaluating a wildfire hazard index. *J. Amer. Statist. Assoc.* **100** 26–35. [MR2166067](#)
- RATHBUN, S. L. and CRESSIE, N. (1994). Asymptotic properties of estimators for the parameters of spatial inhomogeneous Poisson point processes. *Adv. Appl. Probab.* **26** 122–154. [MR1260307](#)
- SCHOENBERG, F. P., BRILLINGER, D. R. and GUTTORP, P. M. (2002). Point processes, spatial-temporal. In *Encyclopedia of Environmetrics* (A. El-Shaarawi and W. Piegorsch, eds.) **3** 1573–1577. Wiley, New York.
- SCHOENBERG, F. P., CHANG, C., KEELEY, J., POMPA, J., WOODS, J. and XU, H. (2010). A critical assessment of the burning Index in Los Angeles County, California. *Int. J. Wildland Fire*. To appear.
- SCHOENBERG, F. P., PENG, R., HUANG, Z. and RUNDEL, P. (2003). Detection of nonlinearities in the dependence of burn area on fuel age and climatic variables. *Int. J. Wildland Fire* **12** 1–10.
- SCHOENBERG, F. P., PENG, R. and WOODS, J. (2003). On the distribution of wildfire sizes. *Environmetrics* **14** 583–592.
- SCHOENBERG, F. P. and XU, H. (2008). Directional kernel regression for wind and fire data. *Environmetrics*. Unpublished manuscript.
- SCHROEDER, M. J., GLOVINSKY, M., HENDRICKS, V., HOOD, F., HULL, M., JACOBSON, H., KIRKPATRICK, R., KRUEGER, D., MALLORY, L., OERTEL, A., REESE, R., SERGIUS, L. and SYVERSON, C. (1964). Synoptic weather types associated with critical fire weather. Institute for Applied Technology, National Bureau of Standards, U.S. Dept. Commerce, Washington, DC.
- SILVERMAN, B. W. (1986). *Kernel Density Estimation and Data Analysis*. Chapman and Hall, London.
- VIEGAS, D. X., BOVIO, G., FERREIRA, A., NOSENZO, A. and SOL, B. (1999). Comparative study of various methods of fire danger evaluation in Southern Europe. *Int. J. Wildland Fire* **9** 235–246.
- WARREN, J. R. and VANCE, D. L. (1981). Remote Automatic Weather Station for Resource and Fire Management Agencies. United States Dept. Agriculture Forest Service Technical Report INT-116. Intermountain Forest and Range Experiment Station.

DEPARTMENT OF STATISTICS
 UNIVERSITY OF CALIFORNIA
 8125 MATH-SCIENCE BUILDING
 LOS ANGELES, CALIFORNIA 90095–1554
 USA
 E-MAIL: xuhy@ucla.edu
frederic@stat.ucla.edu